



Published in final edited form as:

Brain Res. 2015 December 10; 1629: 113–125. doi:10.1016/j.brainres.2015.10.022.

## Glial restricted precursors maintain their permissive properties after long-term expansion but not following exposure to pro-inflammatory factors

Kazuo Hayakawa<sup>1,2</sup>, Christopher Haas<sup>1</sup>, Ying Jin<sup>1</sup>, Julien Bouyer<sup>1</sup>, Takanobu Otsuka<sup>2</sup>, and Itzhak Fischer<sup>1,\*</sup>

<sup>1</sup> Department of Neurobiology and Anatomy, Drexel University College of Medicine, Philadelphia, Pennsylvania, USA

<sup>2</sup> Department of Orthopaedic Surgery, Graduate School of Medical Sciences, Nagoya City University, Nagoya, Japan.

### Abstract

Glial restricted precursors (GRP) are a promising cellular source for transplantation therapy of spinal cord injury (SCI), capable of creating a permissive environment for axonal growth and regeneration. However, there are several issues regarding the nature of their permissive properties that remain unexplored. For example, cellular transplantation strategies for spinal cord repair require the preparation of a large number of cells, but it is unknown whether the permissive properties of GRP are maintained following the process of *in vitro* expansion. We used rat GRP isolated from the embryonic day 13.5 spinal cord to compare the properties of early (10-20 days) and late (120-140 days) passage GRP. We found that late passage GRP showed comparable effects on neurite outgrowth of adult rat DRG to early passage GRP in both *in vitro* co-culture and conditioned medium experiments. In addition, to further examine the effects of the inflammatory cascade activated in the aftermath of SCI on the microenvironment, we studied the direct effects of strong inflammatory mediators, Lipopolysaccharide and interferon gamma (LPS and IFN $\gamma$ ,

\*Corresponding author: Itzhak Fischer, Ph.D., Department of Neurobiology and Anatomy, Drexel University College of Medicine, 2900 Queen Lane, Philadelphia, PA 19129, Tel: +1 215 991 8284, IFischer@drexelmed.edu.  
Kazuo Hayakawa, M.D., Ph.D., Department of Neurobiology and Anatomy, Drexel University College of Medicine, Philadelphia, Pennsylvania, USA; Department of Orthopaedic Surgery, Graduate School of Medical Sciences, Nagoya City University, Nagoya, Japan Tel: +1 215 911 8284 Fax: +1 215 843 9082 kazuo.hayakawa@drexelmed.edu  
Christopher Haas, Department of Neurobiology and Anatomy, Drexel University College of Medicine, Philadelphia, Pennsylvania, USA. Tel: +1 215 991 8284 cjh62@drexel.edu  
Ying Jin, Ph.D., Department of Neurobiology and Anatomy, Drexel University College of Medicine, Philadelphia, Pennsylvania, USA. Tel: +1 215 991 8284 ying.jin@drexelmed.edu  
Julien Bouyer, Department of Neurobiology and Anatomy, Drexel University College of Medicine, Philadelphia, Pennsylvania, USA. Tel: +1 215 991 8284 julien.bouyer@drexelmed.edu  
Takanobu Otsuka, M.D., Ph.D., Department of Orthopaedic Surgery, Graduate School of Medical Sciences, Nagoya City University, Nagoya, Japan Tel: +81 52 853 8236 t.otsuka@med.nagoya-cu.ac.jp  
Itzhak Fischer, Ph.D., Department of Neurobiology and Anatomy, Drexel University College of Medicine, Philadelphia, Pennsylvania, USA. Tel: +1 215 991 8400 Itzhak.fischer@drexelmed.edu

**Publisher's Disclaimer:** This is a PDF file of an unedited manuscript that has been accepted for publication. As a service to our customers we are providing this early version of the manuscript. The manuscript will undergo copyediting, typesetting, and review of the resulting proof before it is published in its final citable form. Please note that during the production process errors may be discovered which could affect the content, and all legal disclaimers that apply to the journal pertain.

**AUTHOR DISCLOSURE**

No conflict of interest.

respectively), on the properties of GRP. We showed that exposure to these pro-inflammatory mediators altered GRP phenotype and attenuated their growth-promoting effects on neurite outgrowth in a dose dependent manner. Taken together, our data suggest that GRP maintain their growth-promoting properties following extensive *in vitro* passaging and underscore the importance of modulating the inflammatory environment at the injured spinal cord.

## Keywords

Spinal cord injury; cell transplantation; DRG neurons; proinflammatory mediators; LPS; Interferon gamma

---

## 1. Introduction

Spinal cord injury (SCI) is a devastating disorder characterized by the disruption of ascending and descending axonal pathways and death of a variety of cells in the central nervous system (CNS) (Simpson et al., 2012; Verma et al., 2008). One of the most significant obstacles for repair following SCI is the inability of injured neurons to regenerate and restore connectivity (Fitch and Silver, 2008). Transplantation of neural progenitors is a promising therapeutic strategy that has the potential to replace lost cells, modulate the inhibitory microenvironment of the CNS, and promote axonal growth (Eftekharpour et al., 2008; Tetzlaff et al., 2011).

Extensive studies using multiple types of cells such as Schwann cells, olfactory ensheathing glial cells, neural stem cells, fate-restricted neural/glial precursor cells, and bone marrow stromal cells have been examined for their therapeutic potential for SCI repair (Falnikar et al., 2014; Lopez-Vales et al., 2006; Medalha et al., 2014; Mendonca et al., 2014). Once appropriate candidates for cell transplantation have been identified, the transition to clinical applications requires culturing and expansion to prepare adequate cell stocks and to determine whether the cells retain their original properties. These are particularly important considerations for primary cells derived from fetal or adult tissue, which unlike embryonic stem (ES)-derived cells, are a limited resource. Several studies have shown that some cells retain their growth-supportive properties following expansion (Akesson et al., 2007; Radtke et al., 2010; Tang et al., 2000; Zhu et al., 2014), but in other cases the transplantation protocols have been restricted to a low cell passage (Huang et al., 2006; Saberi et al., 2008). It is therefore important to define the expansion parameters for specific cell types and use these data to develop appropriate transplantation protocols.

Another issue concerning transplantation following CNS trauma relates to the presence of pro-inflammatory molecules, which are released at the injury site and elicit an immune response leading to astrogliosis and glial scar formation (Donnelly and Popovich, 2008; Fitch and Silver, 2008; Sofroniew, 2009). The inflammatory environment encountered by transplanted cells may produce changes that will affect the phenotypic and functional properties of transplanted cells. These changes can be studied *in vitro* by modeling the direct effects of pro-inflammatory molecules on particular cell types. Lipopolysaccharide (LPS) and interferon gamma (IFN $\gamma$ ) represent powerful, canonical innate inflammatory mediators and have been used extensively to study cellular responses to inflammation (Dafny and

Yang, 2005; Fok-Seang et al., 1998; Fu et al., 2014; Lehnardt et al., 2003). Although the responses of a variety of cell subtypes, such as astrocytes, microglia/ macrophages, and oligodendrocyte precursor cells (OPCs) to inflammation have been previously documented (Tanner et al., 2011; Walter et al., 2011; Zamanian et al., 2012), the changes to the properties of multipotent glial restricted precursors (GRP) following exposure to inflammatory factors has not been examined.

The present report continues our previous studies, which have shown that a combination of neuronal and glial-restricted precursors (NRP/GRP) promoted host axon regeneration of sensory neurons into the injury site to form synaptic connections with transplant-derived neurons and created a function relay across the injury (Bonner et al., 2011; Lepore and Fischer, 2005). The presence of GRP was shown to be a necessary and sufficient component for regeneration, creating a permissive environment even in the presence of inhibitory chondroitin sulfate proteoglycans (CSPGs), a major inhibitory component of the glial scar (See et al., 2010). Conditioned medium harvested from rat GRP also promoted neurite outgrowth of DRG neurons *in vitro*, suggesting that the secretion of soluble factors was responsible the growth (Ketschek et al., 2012).

In the present study we wanted to examine the properties of GRP in the context of their potential application for SCI repair, with specific aims designed to test their ability to support axonal growth following *in vitro* expansion and exposure to inflammatory factors. Here, we demonstrate the consistently permissive nature of late passage GRP (P19-21; grown over 120 days) on neurite outgrowth from adult rat DRG utilizing two experimental protocols, direct DRG-GRP co-culture and the use of conditioned medium, indicating the role of secreted factors. In addition, we examined the direct effects of pro-inflammatory mediators, LPS and IFN $\gamma$ , on the phenotypic and functional properties of GRP with respect to neurite outgrowth using co-culture experiments. This treatment resulted in a reduced capacity to support neurite outgrowth, which correlated with phenotypic changes of GRP. Taken together, these results underscore the therapeutic potential of GRP to serve as permissive cellular transplants in SCI, even after prolonged expansion *in vitro*, but emphasize the importance of the inflammatory microenvironment of the injured spinal cord and its potential influence on the properties of GRP.

## 2. RESULTS

### 2.1. Characterization of late passage GRP

We have previously shown that serum-free defined basal medium supplemented with basic fibroblast growth factor (bFGF) maintains rat GRP in an undifferentiated state for at least 14 days as compared to media supplemented with FBS, BMP-4 or CNTF, which induce differentiation into astrocytes (Haas et al., 2012). Here, we followed a similar culturing method using basal medium supplemented with bFGF, but continued to grow GRP for over 19 passages (ranging from 120 – 140 days *in vitro*) to compare early and late passage GRP with respect to their proliferative potential, morphology, and lineage specific markers. Early passage GRP showed robust proliferation with a population doubling time (PDT:  $22.3 \pm 1.1$  hr), while late passage GRP showed reduced proliferation (PDT:  $27.5 \pm 1.5$  hr), as shown in Figure S1A (see supplemental information). Immunostaining with Ki67, a marker of cell

proliferation, supported these results, showing a large population of cells positive for Ki67 (Figure S1B), with  $60.0 \pm 1.3$  % early passage GRP and  $47.2 \pm 2.4$  % of late passage GRP staining for Ki67 ( $P=0.03$ ). Early passage GRP had a typical morphology of a non-differentiated progenitor characterized by small refractive cell bodies and a short stellate or bipolar appearance (Figure 1A). The vast majority of late passage GRP showed a comparable morphology with only a small number of cells displaying larger cell bodies and multi-branching shapes or cells with a flattened morphology, typical of mature astrocytes (Figure 1E). We have previously described the developmental continuum of GRP (Haas et al., 2012), ranging from immature GRP, characterized by the A2B5 marker, to mature astrocytes characterized by the GFAP marker. Accordingly, early passage GRP showed that  $83.9 \pm 1.5$  % were A2B5+, while  $7.5 \pm 1.3$  % were GFAP+ (Figures 1C-D and I). Of the GFAP+ GRP,  $76.3 \pm 4.2$  % were also A2B5+ (data not shown), indicating that the majority of early passage GRP were in an undifferentiated state. Late passage GRP demonstrated significant changes in A2B5 and GFAP markers, but still retained high levels of A2B5+ of  $51.3 \pm 6.2$  %,  $P=0.04$  relative to early passage GRP (Figure 1D and I) and low levels of GFAP+ ( $25.2 \pm 1.1$  %,  $P=0.03$  relative to early passage GRP) (Figures 1H and I). The A2B5+ cells within the GFAP+ population also remained high and showed a comparable ratio to that of early passage GRP ( $53.9 \pm 3.2$  %,  $P=0.07$ , data not shown). Nestin and Vimentin, stem cell and progenitor markers that are down-regulated in differentiated astrocytes, were expressed in both early and late passage GRP at high levels (Nestin:  $91.9 \pm 2.4$  % and  $96.0 \pm 0.6$  %, ( $P=0.30$ ), Vimentin:  $98.1 \pm 0.3$  % and  $92.9 \pm 2.5$  %, ( $P=0.43$ ), respectively) (Figure 1B, F and I). There were no mature oligodendrocytes or neuronal lineages in either early or late passage cultures as evidenced by the absence of staining for myelin basic protein (MBP) and  $\beta$ III tubulin (Tuj1), respectively. MBP staining was  $0.1 \pm 0.0$  % and  $0.2 \pm 0.0$  %, ( $P=0.47$ ), while Tuj1 staining was  $1.8 \pm 0.1$  % and  $1.7 \pm 0.1$  %, ( $P=0.70$ ), in early and late passage GRP cultures, respectively (Figure 1I). These results indicated that although late passage GRP exhibited a reduced proliferation rate and some phenotypic changes, overall, they maintained their immature/stem cell properties following long-term *in vitro* passaging.

## 2.2. Late Passage GRP still promote neurite outgrowth in vitro

We assessed whether long-term passage of GRP affects their functional properties in an assay designed to examine their ability to support neurite outgrowth of adult DRG neurons. We first used DRG-GRP co-culture experiments and immunostained with specific cell markers to distinguish Tuj1+ DRG neurons from Nestin+/AP+ GRP (Figures 2A-E, G-F and S2A-C) and to quantify the effects of GRP on neurite outgrowth. Early and late passage GRP did not show significant differences in neurite number relative to controls of DRG neurons alone (Control:  $2.945 \pm 0.2122$ , early passage:  $2.866 \pm 0.1950$ , late passage:  $2.625 \pm 0.1481$ ,  $P=1.0$ ), (Figure 2K). In contrast, cultures of early and late passage GRP showed significant differences in the average neurite length and the size of the longest neurite relative to controls; Average neurite length: Control:  $197.4 \pm 11.20$   $\mu$ m, early passage:  $363.5 \pm 21.27$   $\mu$ m ( $P<0.001$ ), late passage:  $444.1 \pm 21.21$   $\mu$ m ( $P<0.001$ ) (Figure 2L); Longest neurite length: Control:  $313.1 \pm 14.70$   $\mu$ m, early passage:  $522.7 \pm 46.75$   $\mu$ m ( $P<0.001$ ), late passage:  $648.2 \pm 55.07$   $\mu$ m ( $P=0.005$ ) (Figure 2M). Importantly, there were no significant

differences between early and late passage GRP with respect to their ability to increase average neurite length and the length of the longest neurite (Figure 2L-M).

We then performed conditioned medium experiments and compared the results of neurite growth between the various conditions, as well as to the DRG-GRP co-culture experiments (Figure 2A, F and J). DRG cultured in conditioned media from early and late passage GRP showed a significant increase in average neurite length and the size of the longest neurite relative to control cultures of DRG neurons alone; Average neurite length: early passage:  $404.1 \pm 25.30 \mu\text{m}$  ( $P < 0.001$ ), late passage:  $411.4 \pm 23.86 \mu\text{m}$  ( $P < 0.001$ ) (Figure 2L); Longest neurite length: early passage:  $603.8 \pm 46.31 \mu\text{m}$  ( $P < 0.001$ ), late passage:  $635.5 \pm 46.21 \mu\text{m}$  ( $P < 0.001$ ) (Figure 2M). In contrast to the results of direct DRG-GRP co-culture experiments, the number of primary neurites from DRG neurons were increased in conditioned medium experiments from both early and late passage GRP relative to controls; early passage:  $4.59 \pm 0.97$  ( $P = 0.009$ ), late passage:  $3.62 \pm 0.06$  ( $P < 0.001$ ), respectively (Figure 2K). As in co-culture studies, conditioned media from early and late passage GRP showed no significant differences in DRG neurite number, average neurite length, or longest neurite length ( $P = 1.0$  in all comparisons) (Figure 2K-M).

Next, we compared the results of direct DRG-GRP co-culture experiments (effects of cell-surface interaction) with results obtained from conditioned medium experiments (effects of secreted factors). Both average neurite length and the length of the longest neurite from early passage GRP conditioned media showed comparable responses to co-culture experiments ( $P = 1.0$ ,  $P = 1.0$ , respectively) (Figure 2L-M). Similarly, conditioned media harvested from late passage GRP showed comparable effects on average neurite length and length of the longest neurite length compared to direct co-culture studies ( $P = 1.0$ ,  $P = 1.0$ , respectively) (Figure 2L-M). In contrast, conditioned medium harvested from early or late passage GRP showed a significant increase in the number of primary neurites relative to those in co-culture experiments (early passage:  $P = 0.001$ , late passage:  $P < 0.001$ ), (Figure 2K). These results indicated that secreted factors from both early and late passage GRP were sufficient to promote neurite outgrowth from DRG with respect to the neurite number, average and longest neurite length. Importantly, the results demonstrated that late passage GRP maintained their permissive properties on neurite outgrowth in both assays.

### **2.3. LPS and IFN $\gamma$ treatment altered the phenotypic properties of GRP distinct from a reactive astrocyte state**

To mimic the inflammatory environment encountered by GRP following transplantation into the injured spinal cord, we next examined the direct effects of LPS and IFN $\gamma$  as pro-inflammatory mediators on the morphological, phenotypic, and functional properties of GRP. First, we confirmed receptor expression for the cognate LPS and IFN $\gamma$  ligands, Toll-like receptor 4 (TLR4) (Lehnardt et al., 2003) and Interferon gamma receptor alpha (IFN $\gamma$ R $\alpha$ ) (Tsuda et al., 2009) respectively, by immunocytochemistry (Figure S3A and B, respectively). To address whether LPS in combination with IFN $\gamma$ , which have been shown to have synergistic effects (Schroder et al., 2006; Yoo et al., 2008), can alter the properties of GRP, we exposed GRP to selected concentrations of these reagents for 24 hr and observed their proliferation and morphology for 8 days. Treatment of GRP with increasing

concentrations of LPS and IFN $\gamma$  (0.1–10  $\mu\text{g/ml}$  of LPS and 0.3–30  $\text{ng/ml}$  of IFN $\gamma$ ) for 24 hr did not induce apparent growth inhibition by 7 days after treatment (Figure 3A). Similarly, analysis of Ki67 staining demonstrated that there was no inhibition of cell division by LPS and IFN $\gamma$  at day 2 and day 5 relative to untreated control; Day2: LPS 0  $\mu\text{g/ml}$  - IFN $\gamma$  0  $\text{ng/ml}$ ,  $63.6 \pm 3.6\%$ ; LPS 0.1  $\mu\text{g/ml}$  - IFN $\gamma$  0.3  $\text{ng/ml}$ ,  $71.2 \pm 3.5\%$  ( $P=0.89$ ); LPS 1.0  $\mu\text{g/ml}$  - IFN $\gamma$  3.0  $\mu\text{g/ml}$ ,  $51.5 \pm 4.0\%$  ( $P=0.22$ ); LPS 10  $\mu\text{g/ml}$  - IFN $\gamma$  30  $\mu\text{g/ml}$ ,  $56.7 \pm 2.5\%$  ( $P=1.0$ ), Figure 3B). Interestingly, although GRP exposed to lower concentrations of LPS and IFN $\gamma$  (LPS 0.1  $\mu\text{g/ml}$  - IFN $\gamma$  0.3  $\text{ng/ml}$ , Figure 3D) did not show morphological changes relative to untreated GRP (Figure 3C), when GRP were exposed to higher concentrations of LPS and IFN $\gamma$  (LPS 1.0  $\mu\text{g/ml}$  - IFN $\gamma$  3.0  $\text{ng/ml}$  and LPS 10  $\mu\text{g/ml}$  - IFN $\gamma$  30  $\text{ng/ml}$ , Figure 3E-F), they developed longer processes one day after treatment. These changes, however, were transient and at day five of the experiment all GRP cultures had an undifferentiated morphology and were indistinguishable from each other (Figure 3G-J). We then examined the phenotypic profiles of GRP following LPS-IFN $\gamma$  treatment and found that GFAP expression was induced in all LPS-IFN $\gamma$  treatment groups at day 2 but returned to control levels at day 5 (Figure 4A-D and M-P) as follows: Day2: Control  $10.8 \pm 0.6\%$ ; LPS 0.1  $\mu\text{g/ml}$  - IFN $\gamma$  0.3  $\mu\text{g/ml}$ ,  $67.3 \pm 1.8\%$  ( $P<0.001$ ); LPS 1.0  $\mu\text{g/ml}$  - IFN $\gamma$  3.0  $\text{ng/ml}$ ,  $47.6 \pm 6.2\%$  ( $P=0.009$ ); LPS 10  $\mu\text{g/ml}$  - IFN $\gamma$  30  $\text{ng/ml}$ ,  $44.7 \pm 5.3\%$  ( $P=0.015$ ); Day5: Control  $4.6 \pm 0.6\%$ ; LPS 0.1  $\mu\text{g/ml}$  - IFN $\gamma$  0.3  $\text{ng/ml}$ ,  $5.2 \pm 1.8\%$ ; LPS 1.0  $\mu\text{g/ml}$  - IFN $\gamma$  3.0  $\text{ng/ml}$ ,  $3.8 \pm 0.5\%$ ; LPS 10  $\mu\text{g/ml}$  - IFN $\gamma$  30  $\text{ng/ml}$ ,  $34.2 \pm 0.4\%$  ( $P=1.0$  in all comparisons) (Figure 4i). Nestin and Vimentin, which were originally expressed in a large proportion of GRP on day 0 did not change during LPS-IFN $\gamma$  treatment (Figure S4). To assess the possibility that high concentrations of LPS-IFN $\gamma$  affected lineage commitment, we performed immunostaining with lineage-specific antibodies. At day 2, A2B5 expression in each group were comparable to untreated GRP, but were down-regulated at higher concentration groups at day 5 (Figure 4E-H, Q-T). A2B5 $^{+}$  expression in GFAP $^{+}$  cells was also decreased in higher concentration groups at day 5 (Figure 4I-L, U-X). Quantitative analysis confirmed a significant decrease of A2B5 $^{+}$  at higher concentrations LPS-IFN $\gamma$  treated groups at day 5 as follows: Control,  $84.9 \pm 1.6\%$ ; LPS 0.1  $\mu\text{g/ml}$  - IFN $\gamma$  0.3  $\text{ng/ml}$ ,  $82.9 \pm 1.2\%$  ( $P=1.0$ ); LPS 1.0  $\mu\text{g/ml}$  - IFN $\gamma$  3.0  $\text{ng/ml}$ ,  $55.6 \pm 0.7\%$  ( $P<0.001$ ); LPS 10  $\mu\text{g/ml}$  - IFN $\gamma$  30  $\text{ng/ml}$ ,  $55.3 \pm 2.6\%$  ( $P<0.001$ ) (Figure 4ii); A2B5 $^{+}$ /GFAP $^{+}$ : Control  $74.7 \pm 4.6\%$ ; LPS 0.1  $\mu\text{g/ml}$  - IFN $\gamma$  0.3  $\text{ng/ml}$ ,  $50.7 \pm 3.9\%$  ( $P=0.54$ ); LPS 1.0  $\mu\text{g/ml}$  - IFN $\gamma$  3.0  $\text{ng/ml}$ ,  $25.4 \pm 2.6\%$  ( $P=0.026$ ); LPS 10  $\mu\text{g/ml}$  - IFN $\gamma$  30  $\text{ng/ml}$ ,  $20.4 \pm 3.5\%$  ( $P=0.015$ ) (Figure 4iii). These population changes, however, were transient and recovered to the level equivalent to untreated GRP by day 8 (data not shown). We also measured cell populations of other lineages such as MBP (oligodendrocytes), Tuj1 (neurons), NG2 (oligodendrocyte precursors), and Iba1 (microglia) but did not find significant changes (Figure S5 and data not shown).

#### 2.4. GRP stimulated with pro-inflammatory mediators attenuated their growth promoting properties

We assessed the effects of LPS-IFN $\gamma$ -treated GRP on neurite outgrowth using our standard DRG-GRP co-culture assays (Fu et al., 2014; Hamby et al., 2012). GRP were exposed to selected concentrations of LPS-IFN $\gamma$  for 24 hr (LPS-IFN $\gamma$ : 0.1-0.3, 1.0-3.0, and 10-30  $\mu\text{g/ml-ng/ml}$ , respectively) and were utilized in phenotypic analyses. Following incubation

cells were washed and cultured with dissociated DRG in CBM for three additional days (Figure 5A). We did not observe DRG cell death in any of the treated groups (Figure 5B-K). There were also no significant differences in primary neurite number, average length, or longest neurite length in DRG co-cultured with GRP treated with low concentrations of LPS-IFN $\gamma$  relative to untreated GRP. Primary neurite number: Control  $4.09 \pm 0.08$ ; LPS 0.1  $\mu\text{g/ml}$  - IFN $\gamma$  0.3 ng/ml,  $4.48 \pm 0.05$  ( $P=1.0$ ); Average length: control,  $693.7 \pm 15.9 \mu\text{m}$ ; LPS 0.1  $\mu\text{g/ml}$  - IFN $\gamma$  0.3 ng/ml,  $823.1 \pm 15.4 \mu\text{m}$  ( $P=0.093$ ); Longest length: Control  $1118.9 \pm 27.9 \mu\text{m}$ ; LPS 0.1  $\mu\text{g/ml}$  - IFN $\gamma$  0.3 ng/ml  $1295.5 \pm 23.1 \mu\text{m}$  ( $P=1.0$ ). However, we found significant attenuation of growth in all three parameters at higher concentrations. Primary neurite number: LPS 1.0  $\mu\text{g/ml}$  - IFN $\gamma$  3.0 ng/ml,  $3.00 \pm 0.06$  ( $P=0.093$ ); LPS 10.0  $\mu\text{g/ml}$  - IFN $\gamma$  30.0 ng/ml,  $2.79 \pm 0.05$  ( $P=0.015$ ); Average length: LPS 1.0  $\mu\text{g/ml}$  - IFN $\gamma$  3.0 ng/ml,  $467.1 \pm 16.1 \mu\text{m}$  ( $P=0.025$ ), LPS 10  $\mu\text{g/ml}$  - IFN $\gamma$  30 ng/ml,  $332.8 \pm 9.8 \mu\text{m}$  ( $P<0.001$ ); Longest length: LPS 1.0  $\mu\text{g/ml}$  - IFN $\gamma$  3.0 ng/ml,  $659.0 \pm 19.6 \mu\text{m}$  ( $P=0.004$ ), LPS 10  $\mu\text{g/ml}$  - IFN $\gamma$  30 ng/ml,  $496.3 \pm 14.8 \mu\text{m}$  ( $P<0.001$ ), as shown in Figure 5L-N. We also performed the same experiments using conditioned medium from GRP stimulated with LPS-IFN $\gamma$  and obtained a similar trend (data not shown). These data indicate that GRP treatment with the pro-inflammatory combination of LPS-IFN $\gamma$  reduces the permissive properties of GRP with respect to promoting neurite outgrowth in a dose dependent manner.

### 3. DISCUSSION

Astrocytes are abundant cells in the CNS (Wang and Bordey, 2008), produced during development by glial progenitors, such as GRP, and provide critical supportive functions for axonal and synaptic connectivity. Such progenitors can be isolated from embryonic tissue and expanded for therapeutic applications to reduce inhibition and provide a permissive environment for neuroprotection and axonal growth (Mothe and Tator, 2013; Okano et al., 2007; Tetzlaff et al., 2011). It is therefore critical to establish efficient culture protocols for large-scale cell preparation, and characterize these cell populations in terms of their phenotypic and functional properties under different environments (Haas et al., 2012; Haas and Fischer, 2013). The present study addresses these issues by analyzing the properties of glial progenitors after long term culturing and following exposure to inflammatory mediators.

#### 3.1. Phenotypic and functional properties of late passage cells

Many of the early studies of cell transplantation for SCI repair have used acutely isolated cells or cells that have been expanded with minimal *in vitro* expansion because of concern about phenotypic and functional changes during long-term culturing and cell passaging (Tetzlaff et al., 2011). For example, a study describing the co-culturing of primary astrocytes isolated from newborn rat cerebral cortices showed increased in neurite outgrowth from E18 rat cerebral cortical and E7 chick retinal neurons (Smith et al., 1990). However, when astrocytes were maintained for a month in the presence of fetal bovine serum, forming “mature cultured astrocytes,” the cells showed an attenuated ability to support neurite outgrowth (Smith et al., 1990). Similarly, olfactory ensheathing cells, specialized glial cells with properties of both Schwann cells and astrocytes, have the potential to proliferate, but showed an impaired ability to remyelinate the injured spinal cord after 6 weeks culture

(Radtke et al., 2010). Alternatively, neural cells can be prepared from stem/progenitor cells, instead of acute primary cultures, with sources ranging from ES cells to multipotent neural stem cells and lineage specific progenitors. For example, OPCs isolated from neonatal rat optic nerve can be cultured continuously for many months without losing their functional properties, but they gradually acquire the characteristics of adult OPCs, suggesting that they have an intrinsic maturation program (Tang et al., 2000). Other studies have shown that OPCs from rat neonatal brain maintained as oligospheres for several months could differentiate into functional oligodendrocytes capable of myelinating axons of primary cortical neurons in a co-culture (Zhu et al., 2014). As an alternative, multipotent neural stem cells derived from embryonic human spinal cord and grown as neurospheres can be successfully expanded for up to 25 passages (> 350 days) *in vitro*. They continue to proliferate and maintain their multipotent differentiation property *in vivo* when grafted into an SCI model (Akesson et al., 2007). These examples emphasize the importance of identifying an appropriate source for derivation and expansion of cells used in transplantation therapy with respect to their developmental continuum. For primary cells, long-term culture of differentiated glial cells induces a maturation process that results in the loss of permissive properties. In contrast, long-term culturing of cells prepared from progenitors such as OPC (Tang et al., 2000) and GRP (current study) appear to retain their original properties despite some phenotypic changes, likely reflecting the self-renewal potential of these cells when grown with mitogens and without differentiation factors for a period of several months. In this sense, using ES or iPS cells can provide an unlimited potential for the initial expansion process, which is proceeded by specific differentiation protocols (Krencik and Zhang, 2011; Sareen et al., 2014). For example, OPC derived from ES cells have been used as cells for transplantation in a clinical trial of SCI initiated by Geron (Alper, 2009).

In this study, we cultured GRP in serum-free, defined media supplemented with bFGF mitogen for over 120 days, and compared the cells from early and late passages with respect to proliferative property, morphology, and differentiation state by lineage marker expression. Late passage GRP were still proliferative, although they showed reduced cell growth compared to early passage GRP, and mostly retained the typical morphology of immature GRP with small refractive cell bodies and a short or bipolar appearance. The phenotypic classification of early and late passage GRP along an immature GRP to differentiated astrocyte spectrum showed that the majority of both early and late passage GRP remained immature, expressing the A2B5 marker, but a small population of late passage GRP began to differentiate into GFAP+ astrocytes. As an indication of a transitional state, the majority of these GFAP+ cells co-expressed the A2B5 marker and nearly 90% also expressed progenitor markers such as Nestin and Vimentin, without evidence of other differentiation markers for oligodendrocytes or neuronal lineage such as MBP or Tuj1, respectively. Taken together, our results indicated that although late passage GRP began a maturation process, they maintained most of the immature characteristics of early passage GRP for 120 days of culturing.

For functional analysis we compared neurite outgrowth from adult rat DRG co-cultured with early or late passage GRP. Both early and late passage cultures significantly promoted neurite outgrowth as measured by average neurite length and the length of the longest



neurite, without affecting neurite number. These comparable effects on growth in average and longest neurite length were also observed in conditioned medium experiments indicating the presence of growth promoting factors secreted by GRP. We, however, observed increased neurite number only from DRG cultured in conditioned media from early and late passage GRP, but not in co-culture. These phenomena may imply the presence of different effects of cell-cell interaction and secreted factors on neurite growth, although possible effect of cells from dissociated DRG (e.g. Schwann cells) has not been completely excluded (Jeon et al., 2011; Park et al., 2012). Taken together, these results indicated that late passage GRP remained in an immature state and maintained their permissive effects on neurite growth, suggesting that these cells can be expanded in the presence of the bFGF mitogen and potentially used for transplantation therapy in the repair of SCI.

### 3.2. Effects of pro-inflammatory mediators

In response to trauma the CNS initiates a cascade of events mediated by inflammatory signaling cascades initially involving resident microglia and astrocytes and later other immune cells. The reactive astrogliosis associated with this process triggers astrocytes to undergo a complex and heterogeneous set of morphological, gene expression, and functional changes that depend on location, severity, and timing following the insult (Fitch and Silver, 2008; Hamby et al., 2012; Yuan and He, 2013). Reactive astrocytes, however, can exert both beneficial and detrimental effects in a context-dependent manner, as determined by the activation of specific molecular signaling cascades (Sofroniew, 2009). DNA microarray analysis revealed temporal changes in the reactive astrocyte transcriptome initiated by either ischemic stroke injury or LPS-induced neuro-inflammation and demonstrated the presence of distinct populations of reactive astrocytes that possess beneficial or detrimental effects (Zamanian et al., 2012).

If GRP are going to be used in treatment of SCI, it is important to understand how such an inflammatory microenvironment affects the grafted cells and whether it will induce changes typical of reactive astrocytes. We therefore examined the direct effects of inflammation on GRP using LPS and IFN $\gamma$  as powerful pro-inflammatory mediators and studied the phenotypic and functional response of the GRP cells. We applied these two agents to maximize the pro-inflammatory effects through independent pathways and synergistic signal integration (Hamby et al., 2012; Schroder et al., 2006; Yoo et al., 2008). This combination treatment could be used because GRP express both TLR4 and IFN $\gamma$ R $\alpha$ , signal transducers of LPS and IFN $\gamma$ , respectively (Lehnardt et al., 2003; Tsuda et al., 2009). However, it is important to note that other molecules associated with the compromised blood-brain barrier, such as albumin and thrombin, can also affect astrocytes and change their morphological and functional properties as part of the pro-inflammatory cascade (Chodobski et al., 2011). In our study, LPS and IFN $\gamma$  treatment of GRP did not induce apparent cell growth arrest, but when treated with high concentrations, the cells transiently changed their morphology to cells with long processes. In addition, GFAP expression was induced immediately after treatment even at low concentration of LPS and IFN $\gamma$ , but the expression was transient and disappeared at day 5. Interestingly, the GFAP expression induced by LPS and IFN $\gamma$  was accompanied by co-expression of the immature A2B5 marker, which was diminished only when GRP were treated with high concentrations of the pro-inflammatory agents. These

results suggest that the effects of LPS and IFN $\gamma$  on GRP (e.g. induced GFAP, reduced A2B5 expression) were the result of direct pro-inflammatory signaling, acting in a dose dependent manner.

Previous studies have shown that treatment of OPC with IFN $\gamma$  arrested their cell cycle, inhibited them from generating oligodendrocytes and increased their tendency to generate GFAP+ astrocytes. These results suggest that OPC (which are similar to GRP) withstand inflammation and respond by differentiating into astrocytes (Dafny and Yang, 2005). Application of IFN $\gamma$  to mouse NSC induced developmentally atypical GFAP expression along with neural stem cell markers and prevented normal differentiation (Walter et al., 2011). It appears therefore that the GFAP expression observed in this study may be induced by IFN $\gamma$  and represent either a direct effect on gene expression or the early stages of astrocyte differentiation. The effects of LPS are mediated through TLR and represent the first step of innate immune cell activation. TLR signaling in astrocyte activation is not well understood but they appear to mediate the pro-inflammatory response by the interplay between NF $\kappa$ B, MAPK, and Jak1/Stat1 signaling pathways (Gorina et al., 2011). Modulation of this signaling may affect the various functional responses of astrocytes in CNS injury, some of which are beneficial (Sofroniew, 2009). In contrast, LPS appear to be detrimental to oligodendrocytes, inducing cell death and demyelination (Felts et al., 2005).

To examine whether LPS/IFN $\gamma$  treatment altered the ability of GRP to promote neurite outgrowth, we used our standardized DRG-GRP co-culture assay. Importantly, high concentrations of LPS/IFN $\gamma$  that induce phenotypic alteration in GRP dramatically attenuated their supportive effects on neurite outgrowth with respect to neurite number, average neurite length, and the length of the longest neurite. To eliminate the possibility of contaminating microglia, which could mediate inflammation and induce neurotoxicity, we stained with the ED1/Iba1 marker and found no positive cells (data not shown). Thus, we confirmed that LPS/IFN $\gamma$  can phenotypically alter GRP and at high concentrations abolish their permissive properties with respect to neurite growth. This result may reflect the conditions observed during the peak of the inflammatory process and astrogliosis (Yang et al., 2005).

#### 4. Conclusions

As a promising candidate for therapeutic intervention in CNS injury, we examined the ability of GRP ability to support axon growth following *in vitro* expansion (designed to achieve enough cells for transplantation) and exposure to inflammatory factors (designed to test their properties at the injury site). We have shown that even after 120 days in culture GRP maintained their permissive characteristics in an assay of neurite outgrowth from adult DRG underscoring the advantages of using progenitors for derivation of immature astrocytes. Exposure of GRP to the pro-inflammatory combination of LPS and IFN $\gamma$  at high concentrations attenuated their growth-promoting effects underscoring the importance of modulating the inflammatory environment of the injured CNS. This study demonstrates the value of the *in vitro* co-culture system for testing and screening the properties of cells and then applying the lessons gained from *in vitro* evaluation for effective transplantation

protocols. These lessons highlight the ability of GRP to support axon growth following *in vitro* expansion and the consequences of their exposure to inflammatory factors.

## 5. Experimental Procedure

### 5.1. GRP cultures

Rat GRP were harvested from embryonic day 13.5 spinal cords of transgenic Fischer-344 rats expressing the human placental alkaline phosphatase (AP) reporter (Akiyama et al., 2004), and prepared as previously described. (Haas et al., 2012) GRP were cultured on Poly-L-Lysine (PLL; 15 mg/ml; Sigma-Aldrich) and Laminin (LN; 15 mg/ml; Invitrogen) coated dishes in GRP culture basal medium (CBM; DMEM-F12 (Gibco), B27 supplement (20 µl/ml; Gibco), N2 supplement (10 µl/ml; Gibco), Pen-Strep (1000 IU/ml; Gibco), BSA (1 mg/ml; Sigma-Aldrich)) supplemented with 30 ng/ml of bFGF (Peprotech) at 37°C in a 5% CO<sub>2</sub> incubator. GRP were cultured for 2-3 passages (grown for 10-20 days *in vitro*; *Early passage*) or 19-21 passages (grown for 120-140 days *in vitro*; *Late passage*) prior to harvest and use in subsequent experiments.

### 5.2. Phenotypic characterization of cultured GRP

To determine the cellular phenotypes of early and late passage GRP, we performed immunocytochemical staining with following cell type specific antibodies for A2B5: glial precursors, Glial fibrillary acid protein (GFAP): astrocytes, Nestin and Vimentin: immature progenitors, respectively, Myelin basic protein (MBP): oligodendrocytes,  $\beta$ III tubulin (Tuj1): neuronal cells, and Ki67: proliferating cells, followed by the appropriately conjugated second antibodies (see Table 1 for detailed information). Cells were fixed with 4% Paraformaldehyde (Electron Microscopy Services). Live staining with primary and secondary antibodies was performed for A2B5 prior to fixation and staining with other antibodies as previously described (Haas et al., 2012). Immunostaining was visualized using a Leica DM5500B fluorescent microscope (Leica Microsystems) with a Retiga-SRV camera (QImaging) or a Leica SP2 AOBS VIS/405 confocal microscope (Leica Microsystems). For quantification of *in vitro* staining, cells from at least three randomly selected fields per coverslip were counted. A minimal of 300 cells per coverslips were counted for each condition with a total of three different coverslips counted per condition. Counting was performed using Slidebook software, ver.4.2 (Olympus) and cells stained with each marker were expressed as percentage of the total number of DAPI+ cells. Each experiment was performed in triplicate.

### 5.3. Treatment of GRP with pro-inflammatory mediators

To address how the inflammatory micro-environment alters the phenotypic characteristics of GRP, we exposed GRP to Lipopolysaccharide (LPS: serotype O127; Sigma) and Interferon gamma (IFN $\gamma$ ; R&D) in selected concentrations in CBM, (LPS - IFN $\gamma$  : 0.1 - 0.3, 1.0 - 3.0, and 10 - 30 µg/ml - ng/ml, respectively), or CBM only as experimental control (LPS - IFN $\gamma$ ; 0 - 0 µg/ml - ng/ml) for 24 hrs. Early passage GRP were plated and maintained for appropriate culture periods, and then LPS and IFN $\gamma$  were added to CBM in the presence of bFGF. After exposure, cells were washed two times for three minutes in CBM and utilized in further experiments.

For analyses with respect to morphology, proliferative capacity, and phenotypic changes of GRP after LPS and IFN $\gamma$  treatment, cells were plated at a density of 1000 cells/cm<sup>2</sup> and maintained in CBM supplemented with bFGF without reaching confluency during the assays. On the day following plating, cells were exposed to LPS and IFN $\gamma$  for 24 hrs. Media was changed every two days after LPS and IFN exposure and cell numbers were counted at days 1, 3, 5, and 8, and immunostaining was performed on fixed cells at days 2, 5, and 8. Staining and counting was performed as described above (section 5.2.). Each experiment was performed in triplicate on three separate occasions.

#### 5.4. Dissociated DRG cultures

Primary dorsal root ganglia were prepared from adult Sprague-Dawley rats as described previously (Jang et al., 2008). Dissociated DRG were utilized in the following experiments: i) DRG-GRP co-culture, ii) GRP conditioned media, and iii) DRG-GRP co-culture using GRP pre-treated with LPS and IFN $\gamma$ .

#### 5.5. DRG-GRP co-cultures

- i) DRG-GRP co-culture experiments were prepared by plating 200 dissociated DRG/well onto 24 well plates coated with PLL/LN or onto monolayer cultures of early passage or late passage GRP prepared three days earlier. GRP were plated at a density of 25,000 cells/cm<sup>2</sup>. DRG were suspended in CBM without any growth factors and plated into wells.
- ii) Conditioned medium was collected from cultures of both early and late passage GRP. Briefly, early or late passage GRP were plated at 25,000 cells/cm<sup>2</sup> and cultured for two days in CBM supplemented with 30 ng/ml bFGF. Media was then removed and cells were washed once with warmed HBSS (Gibco). CBM without additional growth factors was added and incubated for an additional 24hrs. On the following day, medium was harvested and utilized as conditioned medium for further experiments. Dissociated DRG were suspended in conditioned medium from early or late passage GRP culture or in CBM without any growth factors as an experimental control.
- iii) In DRG-GRP co-culture experiments using GRP pre-treated with LPS and IFN $\gamma$ , early passage GRP were exposed to LPS and IFN $\gamma$  two days after plating. Following 24hrs exposure, cells were washed and DRG, suspended in CBM, were added. DRG-GRP co-cultures and DRG cultures with conditioned medium were maintained for three days without any media changes and subsequently prepared for immunocytochemistry. Each experiment was performed in triplicate on three separate occasions.

#### 5.6. Analysis of neurite growth

For measurement of neurite growth, cells were fixed and stained with cell type specific antibodies for Tuj1 and Nestin to distinguish neurons from GRP and other satellite cells. A minimum of 30 of Tuj1+ soma with neurite longer than 20 $\mu$ m were chosen in randomly selected fields and utilized for further analysis. Counting was performed manually with

Slidebook software by a blinded observer. Average neurite length, longest neurite length, and primary neurite number were measured using NeuronJ software, ver. 1.4.2.

### 5.7. Statistical analysis

All data are expressed as mean  $\pm$  standard error of the mean (SEM). Statistical analysis was performed using SPSS statistical software using student T-test and one-way ANOVA followed by Bonferroni test for multiple comparisons. Significance was set at  $P < 0.05$ .

## Supplementary Material

Refer to Web version on PubMed Central for supplementary material.

## ACKNOWLEDGMENTS

We thank B. T. Himes, T. Connors, M. P. Cote, X. Yuan, V. Zhukarev, L. Zholudeva, S. Pandey, for their invaluable comments and discussion, M. Obrocka for experimental management and technical assistance. KH is thankful to Ayano Hayakawa for constant encouragement and support during this study. This work was supported by the Craig H. Neilsen Foundation and the NIH grant NS055976.

## ABBREVIATIONS

<b>GRP</b>	Glial restricted precursors
<b>SCI</b>	Spinal cord injury
<b>LPS</b>	Lipopolysaccharide
<b>IFN<math>\gamma</math></b>	Interferon gamma
<b>OPC</b>	oligodendrocyte precursor cell
<b>NRP</b>	Neuronal restricted precursors
<b>ES cells</b>	embryonic stem cells
<b>TRL4</b>	Toll-like receptor 4
<b>IFN<math>\gamma</math>R<math>\alpha</math></b>	Interferon gamma receptor alpha

## REFERENCES

- Akesson E, Piao JH, Samuelsson EB, Holmberg L, Kjaeldgaard A, Falci S, Sundstrom E, Seiger A. Long-term culture and neuronal survival after intraspinal transplantation of human spinal cord-derived neurospheres. *Physiol Behav.* 2007; 92:60–6. [PubMed: 17610915]
- Akiyama Y, Lankford K, Radtke C, Greer CA, Kocsis JD. Remyelination of spinal cord axons by olfactory ensheathing cells and Schwann cells derived from a transgenic rat expressing alkaline phosphatase marker gene. *Neuron Glia Biol.* 2004; 1:47–55. [PubMed: 16799702]
- Alper J. Geron gets green light for human trial of ES cell-derived product. *Nat Biotechnol.* 2009; 27:213–4. [PubMed: 19270655]
- Bonner JF, Connors TM, Silverman WF, Kowalski DP, Lemay MA, Fischer I. Grafted neural progenitors integrate and restore synaptic connectivity across the injured spinal cord. *J Neurosci.* 2011; 31:4675–86. [PubMed: 21430166]

- Chodobski A, Zink BJ, Szmydynger-Chodobska J. Blood-brain barrier pathophysiology in traumatic brain injury. *Transl Stroke Res.* 2011; 2:492–516. [PubMed: 22299022]
- Dafny N, Yang PB. Interferon and the central nervous system. *Eur J Pharmacol.* 2005; 523:1–15. [PubMed: 16226745]
- Donnelly DJ, Popovich PG. Inflammation and its role in neuroprotection, axonal regeneration and functional recovery after spinal cord injury. *Exp Neurol.* 2008; 209:378–88. [PubMed: 17662717]
- Eftekharpour E, Karimi-Abdolrezaee S, Fehlings MG. Current status of experimental cell replacement approaches to spinal cord injury. *Neurosurg Focus.* 2008; 24:E19. [PubMed: 18341395]
- Falnikar A, Li K, Lepore AC. Therapeutically targeting astrocytes with stem and progenitor cell transplantation following traumatic spinal cord injury. *Brain Res.* 2014
- Felts PA, Woolston AM, Fernando HB, Asquith S, Gregson NA, Mizzi OJ, Smith KJ. Inflammation and primary demyelination induced by the intraspinal injection of lipopolysaccharide. *Brain.* 2005; 128:1649–66. [PubMed: 15872019]
- Fitch MT, Silver J. CNS injury, glial scars, and inflammation: Inhibitory extracellular matrices and regeneration failure. *Exp Neurol.* 2008; 209:294–301. [PubMed: 17617407]
- Fok-Seang J, DiProspero NA, Meiners S, Muir E, Fawcett JW. Cytokine-induced changes in the ability of astrocytes to support migration of oligodendrocyte precursors and axon growth. *Eur J Neurosci.* 1998; 10:2400–15. [PubMed: 9749768]
- Fu HQ, Yang T, Xiao W, Fan L, Wu Y, Terrando N, Wang TL. Prolonged neuroinflammation after lipopolysaccharide exposure in aged rats. *PLoS One.* 2014; 9:e106331. [PubMed: 25170959]
- Gorina R, Font-Nieves M, Marquez-Kisinousky L, Santalucia T, Planas AM. Astrocyte TLR4 activation induces a proinflammatory environment through the interplay between MyD88-dependent NFkappaB signaling, MAPK, and Jak1/Stat1 pathways. *Glia.* 2011; 59:242–55. [PubMed: 21125645]
- Haas C, Neuhuber B, Yamagami T, Rao M, Fischer I. Phenotypic analysis of astrocytes derived from glial restricted precursors and their impact on axon regeneration. *Exp Neurol.* 2012; 233:717–32. [PubMed: 22101004]
- Haas C, Fischer I. Human astrocytes derived from glial restricted progenitors support regeneration of the injured spinal cord. *J Neurotrauma.* 2013; 30:1035–52. [PubMed: 23635322]
- Hamby ME, Coppola G, Ao Y, Geschwind DH, Khakh BS, Sofroniew MV. Inflammatory mediators alter the astrocyte transcriptome and calcium signaling elicited by multiple G-protein-coupled receptors. *J Neurosci.* 2012; 32:14489–510. [PubMed: 23077035]
- Huang H, Chen L, Wang H, Xi H, Gou C, Zhang J, Zhang F, Liu Y. Safety of fetal olfactory ensheathing cell transplantation in patients with chronic spinal cord injury. A 38-month follow-up with MRI. *Zhongguo Xiu Fu Chong Jian Wai Ke Za Zhi.* 2006; 20:439–43. [PubMed: 16683452]
- Jang I, La JH, Kim GT, Lee JS, Kim EJ, Lee ES, Kim SJ, Seo JM, Ahn SH, Park JY, Hong SG, Kang D, Han J. Single-Channel Recording of TASK-3-like K Channel and Up-Regulation of TASK-3 mRNA Expression after Spinal Cord Injury in Rat Dorsal Root Ganglion Neurons. *Korean J Physiol Pharmacol.* 2008; 12:245–51. [PubMed: 19967063]
- Jeon EJ, Xu N, Xu L, Hansen MR. Influence of central glia on spiral ganglion neuron neurite growth. *Neuroscience.* 2011; 177:321–34. [PubMed: 21241783]
- Ketschek AR, Haas C, Gallo G, Fischer I. The roles of neuronal and glial precursors in overcoming chondroitin sulfate proteoglycan inhibition. *Exp Neurol.* 2012; 235:627–37. [PubMed: 22498104]
- Krencik R, Zhang SC. Directed differentiation of functional astroglial subtypes from human pluripotent stem cells. *Nat Protoc.* 2011; 6:1710–7. [PubMed: 22011653]
- Lehnardt S, Massillon L, Follett P, Jensen FE, Ratan R, Rosenberg PA, Volpe JJ, Vartanian T. Activation of innate immunity in the CNS triggers neurodegeneration through a Toll-like receptor 4-dependent pathway. *Proc Natl Acad Sci U S A.* 2003; 100:8514–9. [PubMed: 12824464]
- Lepore AC, Fischer I. Lineage-restricted neural precursors survive, migrate, and differentiate following transplantation into the injured adult spinal cord. *Exp Neurol.* 2005; 194:230–42. [PubMed: 15899260]
- Lopez-Vales R, Fores J, Verdu E, Navarro X. Acute and delayed transplantation of olfactory ensheathing cells promote partial recovery after complete transection of the spinal cord. *Neurobiol Dis.* 2006; 21:57–68. [PubMed: 16051494]

- Medalha CC, Jin Y, Yamagami T, Haas C, Fischer I. Transplanting neural progenitors into a complete transection model of spinal cord injury. *J Neurosci Res.* 2014; 92:607–18. [PubMed: 24452691]
- Mendonca MV, Larocca TF, Souza BS, Villarreal CF, Silva LF, Matos AC, Novaes MA, Bahia CM, Martinez AC, Kaneto CM, Furtado SB, Sampaio GP, Soares MB, Dos Santos RR. Safety and neurological assessments after autologous transplantation of bone marrow mesenchymal stem cells in subjects with chronic spinal cord injury. *Stem Cell Res Ther.* 2014; 5:126. [PubMed: 25406723]
- Mothe AJ, Tator CH. Review of transplantation of neural stem/progenitor cells for spinal cord injury. *Int J Dev Neurosci.* 2013; 31:701–13. [PubMed: 23928260]
- Okano H, Kaneko S, Okada S, Iwanami A, Nakamura M, Toyama Y. Regeneration-based therapies for spinal cord injuries. *Neurochem Int.* 2007; 51:68–73. [PubMed: 17544171]
- Park J, Koito H, Li J, Han A. Multi-compartment neuron-glia co-culture platform for localized CNS axon-glia interaction study. *Lab Chip.* 2012; 12:3296–304. [PubMed: 22828584]
- Radtke C, Lankford KL, Wewetzer K, Imaizumi T, Fodor WL, Kocsis JD. Impaired spinal cord remyelination by long-term cultured adult porcine olfactory ensheathing cells correlates with altered in vitro phenotypic properties. *Xenotransplantation.* 2010; 17:71–80. [PubMed: 20149190]
- Saberi H, Moshayedi P, Aghayan HR, Arjmand B, Hosseini SK, Emami-Razavi SH, Rahimi-Movaghgar V, Raza M, Firouzi M. Treatment of chronic thoracic spinal cord injury patients with autologous Schwann cell transplantation: an interim report on safety considerations and possible outcomes. *Neurosci Lett.* 2008; 443:46–50. [PubMed: 18662744]
- Sareen D, Gowing G, Sahabian A, Staggenborg K, Paradis R, Avalos P, Latter J, Ornelas L, Garcia L, Svendsen CN. Human induced pluripotent stem cells are a novel source of neural progenitor cells (iNPCs) that migrate and integrate in the rodent spinal cord. *J Comp Neurol.* 2014; 522:2707–28. [PubMed: 24610630]
- Schroder K, Sweet MJ, Hume DA. Signal integration between IFN $\gamma$  and TLR signalling pathways in macrophages. *Immunobiology.* 2006; 211:511–24. [PubMed: 16920490]
- See J, Bonner J, Neuhuber B, Fischer I. Neurite Outgrowth of Neural Progenitors in Presence of Inhibitory Proteoglycans. *JURNAL OF NEUROTRAUMA.* 2010; 27:951–957.
- Simpson LA, Eng JJ, Hsieh JT, Wolfe DL, Spinal Cord Injury Rehabilitation Evidence Scire Research, T. The health and life priorities of individuals with spinal cord injury: a systematic review. *J Neurotrauma.* 2012; 29:1548–55. [PubMed: 22320160]
- Smith GM, Rutishauser U, Silver J, Miller RH. Maturation of astrocytes in vitro alters the extent and molecular basis of neurite outgrowth. *Dev Biol.* 1990; 138:377–90. [PubMed: 2318341]
- Sofroniew MV. Molecular dissection of reactive astrogliosis and glial scar formation. *Trends Neurosci.* 2009; 32:638–47. [PubMed: 19782411]
- Tang DG, Tokumoto YM, Raff MC. Long-term culture of purified postnatal oligodendrocyte precursor cells. Evidence for an intrinsic maturation program that plays out over months. *J Cell Biol.* 2000; 148:971–84. [PubMed: 10704447]
- Tanner DC, Cherry JD, Mayer-Proschel M. Oligodendrocyte progenitors reversibly exit the cell cycle and give rise to astrocytes in response to interferon-gamma. *J Neurosci.* 2011; 31:6235–46. [PubMed: 21508246]
- Tetzlaff W, Okon EB, Karimi-Abdolrezaee S, Hill CE, Sparling JS, Plemel JR, Plunet WT, Tsai EC, Baptiste D, Smithson LJ, Kawaja MD, Fehlings MG, Kwon BK. A Systematic Review of Cellular Transplantation Therapies for Spinal Cord Injury. *J of Neurotrauma.* 2011; 28:1611–1628. [PubMed: 20146557]
- Tsuda M, Masuda T, Kitano J, Shimoyama H, Tozaki-Saitoh H, Inoue K. IFN-gamma receptor signaling mediates spinal microglia activation driving neuropathic pain. *Proc Natl Acad Sci U S A.* 2009; 106:8032–7. [PubMed: 19380717]
- Verma P, Garcia-Alias G, Fawcett JW. Spinal cord repair: bridging the divide. *Neurorehabil Neural Repair.* 2008; 22:429–37. [PubMed: 18487422]
- Walter J, Honsek SD, Illes S, Wellen JM, Hartung HP, Rose CR, Dihne M. A new role for interferon gamma in neural stem/precursor cell dysregulation. *Mol Neurodegener.* 2011; 6:18. [PubMed: 21371330]
- Wang DD, Bordey A. The astrocyte odyssey. *Prog Neurobiol.* 2008; 86:342–67. [PubMed: 18948166]

- Yang L, Jones NR, Blumbergs PC, Van Den Heuvel C, Moore EJ, Manavis J, Sarvestani GT, Ghabriel MN. Severity-dependent expression of pro-inflammatory cytokines in traumatic spinal cord injury in the rat. *J Clin Neurosci*. 2005; 12:276–84. [PubMed: 15851082]
- Yoo BK, Choi JW, Shin CY, Jeon SJ, Park SJ, Cheong JH, Han SY, Ryu JR, Song MR, Ko KH. Activation of p38 MAPK induced peroxynitrite generation in LPS plus IFN-gamma-stimulated rat primary astrocytes via activation of iNOS and NADPH oxidase. *Neurochem Int*. 2008; 52:1188–97. [PubMed: 18289732]
- Yuan YM, He C. The glial scar in spinal cord injury and repair. *Neurosci Bull*. 2013; 29:421–35. [PubMed: 23861090]
- Zamanian JL, Xu L, Foo LC, Nouri N, Zhou L, Giffard RG, Barres BA. Genomic analysis of reactive astrogliosis. *J Neurosci*. 2012; 32:6391–410. [PubMed: 22553043]
- Zhu B, Zhao C, Young FI, Franklin RJ, Song B. Isolation and long-term expansion of functional, myelinating oligodendrocyte progenitor cells from neonatal rat brain. *Curr Protoc Stem Cell Biol*. 2014; 31:2D 17 1–2D 17 15.



**HIGHLIGHTS**

- GRP promoted neurite outgrowth of DRG using co-cultures and conditioned media
- Late passage GRP (grown for 120 days) maintained growth-promoting effects
- Treatment of GRP with inflammatory factors (LPS/IFN $\gamma$ ) attenuated growth-promoting effects
- Transplants of GRP could potentially be used even after prolonged *in vitro* expansion
- Modulating the inflammatory environment in the aftermath of injury could improve the efficacy of GRP transplants

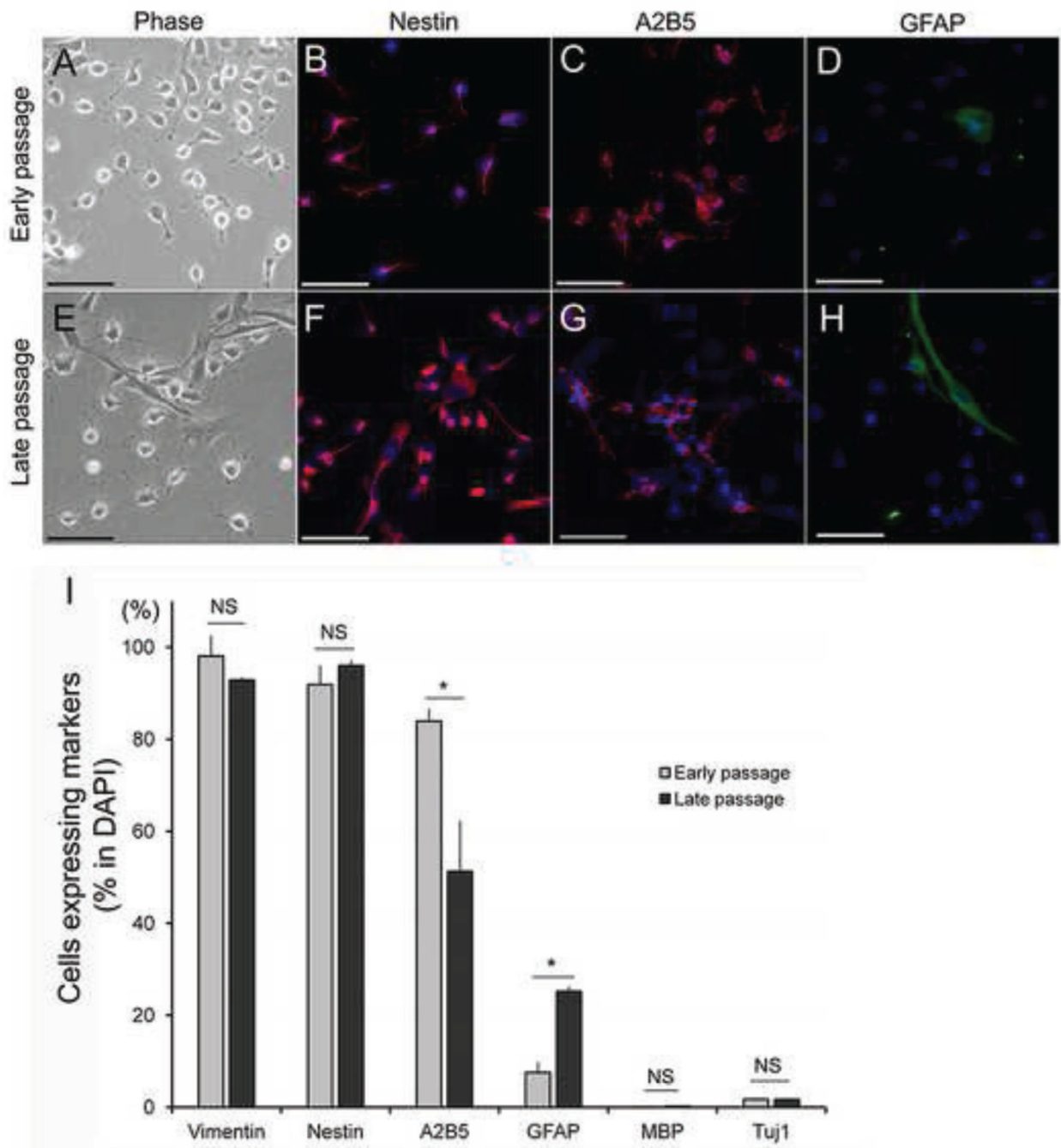


**Figure 1.**

Phenotypic analysis of early and late passage GRP. Early passage GRP showed small refractive cell bodies and a short stellate or bipolar appearance (A), while a majority of late passage GRP showed comparable morphology with only a small number of cells displaying larger cell bodies and multi branching shapes or cell with flattened morphology, typical of mature astrocytes (F). Quantitative analysis using immunostaining demonstrated that late passage GRP showed astrocyte lineage commitment (increase of GFAP+ and decrease of A2B5+) but still kept immature phenotype (high in Vimentin+ and Nestin+) (B-D, F-G and

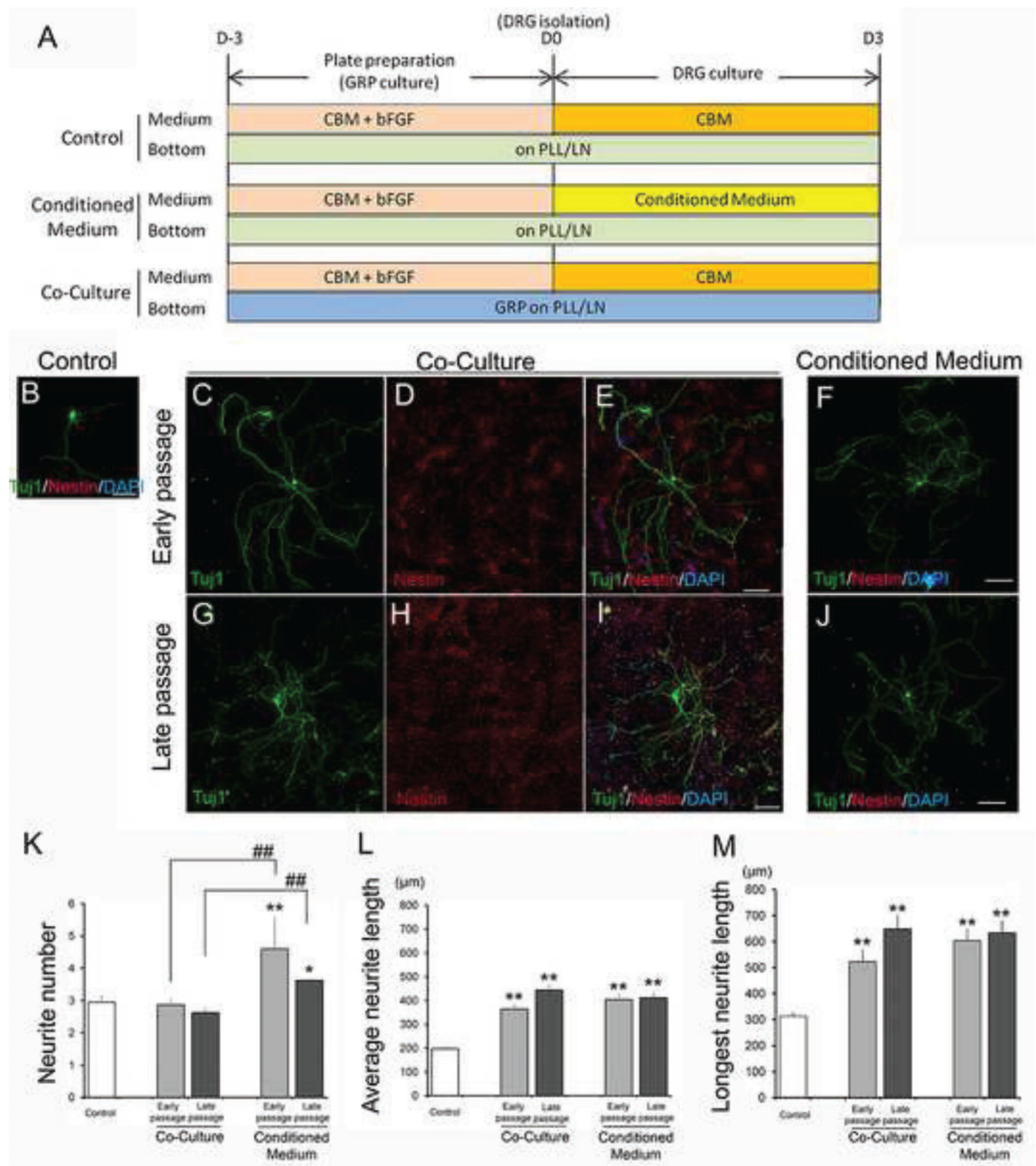
I). Data are presented in graph as mean  $\pm$  standard error of the mean (SEM). Asterisk represents significant difference relative in comparison between early and late passage GRP (Student T-test, \*P<0.05, \*\*P<0.005). Scale bar = 50 $\mu$ m

Author Manuscript

Author Manuscript

Author Manuscript

Author Manuscript

**Figure 2.**

Analysis of the growth-promoting effects on neurite outgrowth from DRG in early and late passage GRP. (A) Experimental design of co-culture and culture with conditioned medium. Immunostaining of DRG in control of DRG alone (B), co-culture with early (C-E) and late passage GRP (G-I), and in conditioned media from early (F) and late passage GRP (J). Scale bars = 150µm. Quantitative analysis of growth-promoting effects on neurite outgrowth from DRG in early and late passage GRP; (K) Primary neurite number, (L) Average neurite length, (M) Longest neurite length are shown in each graph. Asterisk represents significant

differences relative to control (\* $P < 0.05$ , \*\* $P < 0.005$ ). Pound sign represents significant differences relative to correspondents between co-culture and conditioned medium group (# $P < 0.05$ , ## $P < 0.005$ ). Experiments were repeated three times and representative data are shown as mean  $\pm$  standard error of the mean (SEM). Statistical analysis was performed by one-way ANOVA with Bonferroni test ( $N > 70$ ).

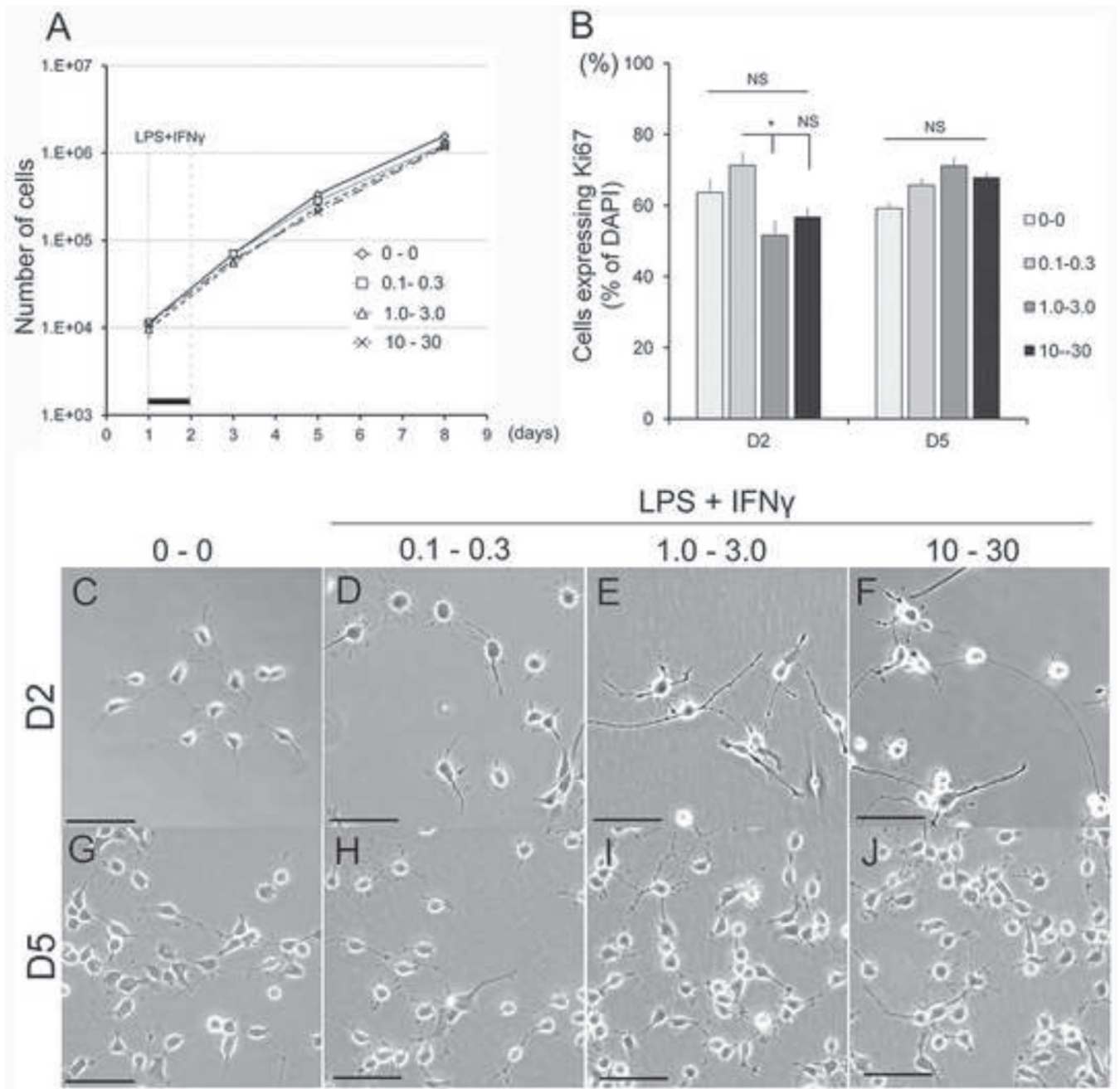


**Figure 3.** Effect of LPS/IFN $\gamma$  on GRP morphology and proliferation. (A) Growth curve of GRPs after LPS/IFN $\gamma$  exposure. Black bar represents time window of LPS/IFN $\gamma$  treatment. (B) Quantitative analysis of Ki67+ cell population after LPS/IFN $\gamma$  treatment. Asterisk represents significant difference relative (\*P<0.05). (C-J) Morphology of GRP at each time point after exposure to LPS/IFN $\gamma$  with different concentrations. Experiments were repeated for three times and representative data are shown in Figures as mean  $\pm$  standard error of the mean (SEM). Statistical analysis was performed by one-way ANOVA with Bonferroni test. Scale bar = 50  $\mu$ m.

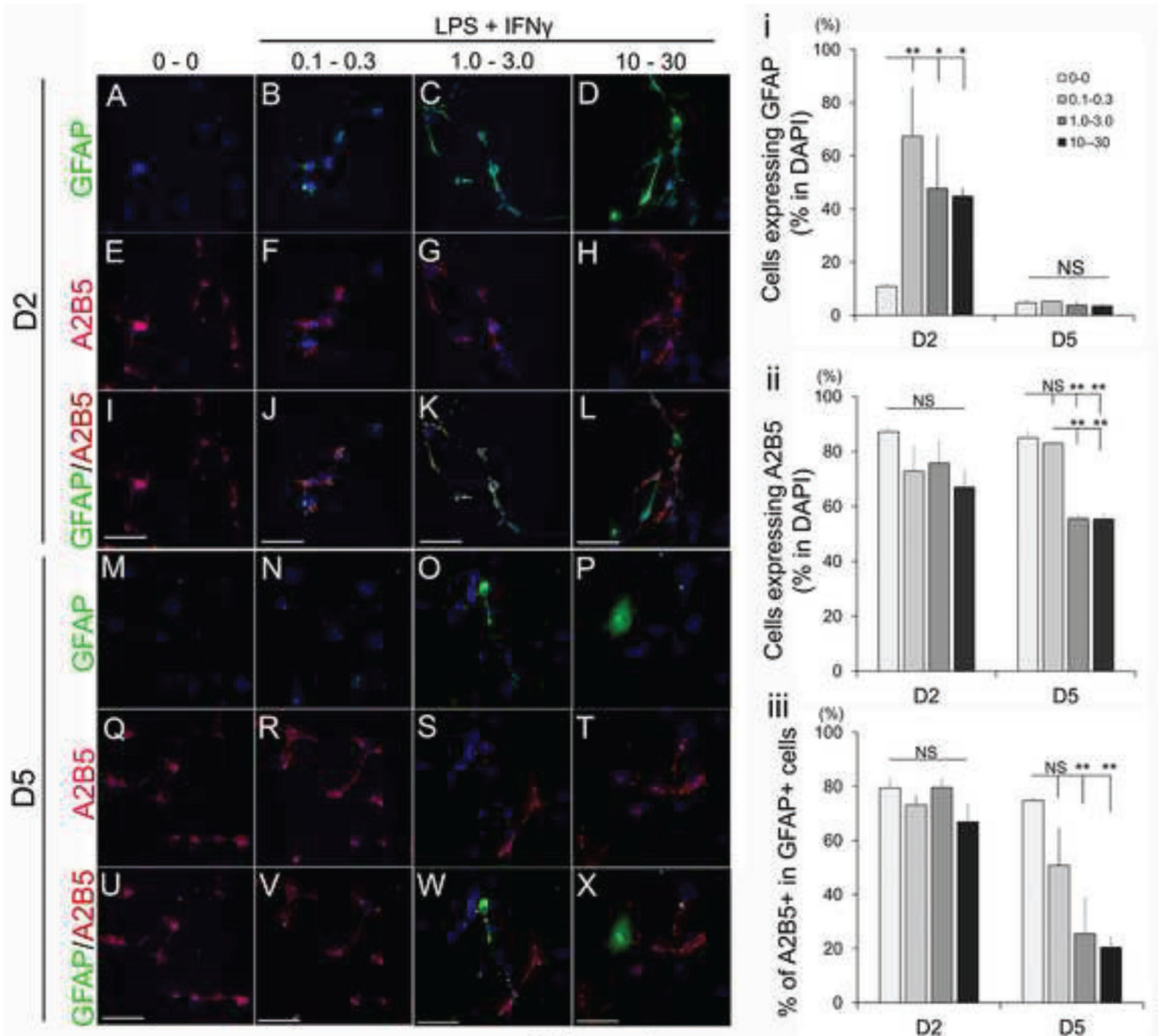


**Figure 4.**

Phenotypic analysis of GRP after LPS/IFN treatment. Immunostaining with antibodies for GFAP and A2B5. GFAP expression was transiently induced at day 2 by LPS/IFN treatment in all concentrations (A-D and M-P), while A2B5 expression was diminished at day 5 only in higher concentration of LPS/IFN (E-L and Q-X). Scale bar = 50 $\mu$ m. (i-iii) Quantitative analysis of GFAP and A2B5+ populations in LPS/IFN treated GRP. Cells with each marker expression were represented as relative to DAPI+ cells (i and ii) and A2B5+ cells in GFAP+ cells (iii) at day 2 and 5. Asterisk indicates significant difference relative to untreated GRP (\* $P$ <0.05, \*\* $P$ <0.005). Experiments were repeated for three times and representative data are shown in Figure as mean  $\pm$  standard error of the mean (SEM). Statistical analysis was performed by one-way ANOVA with Bonferroni test.

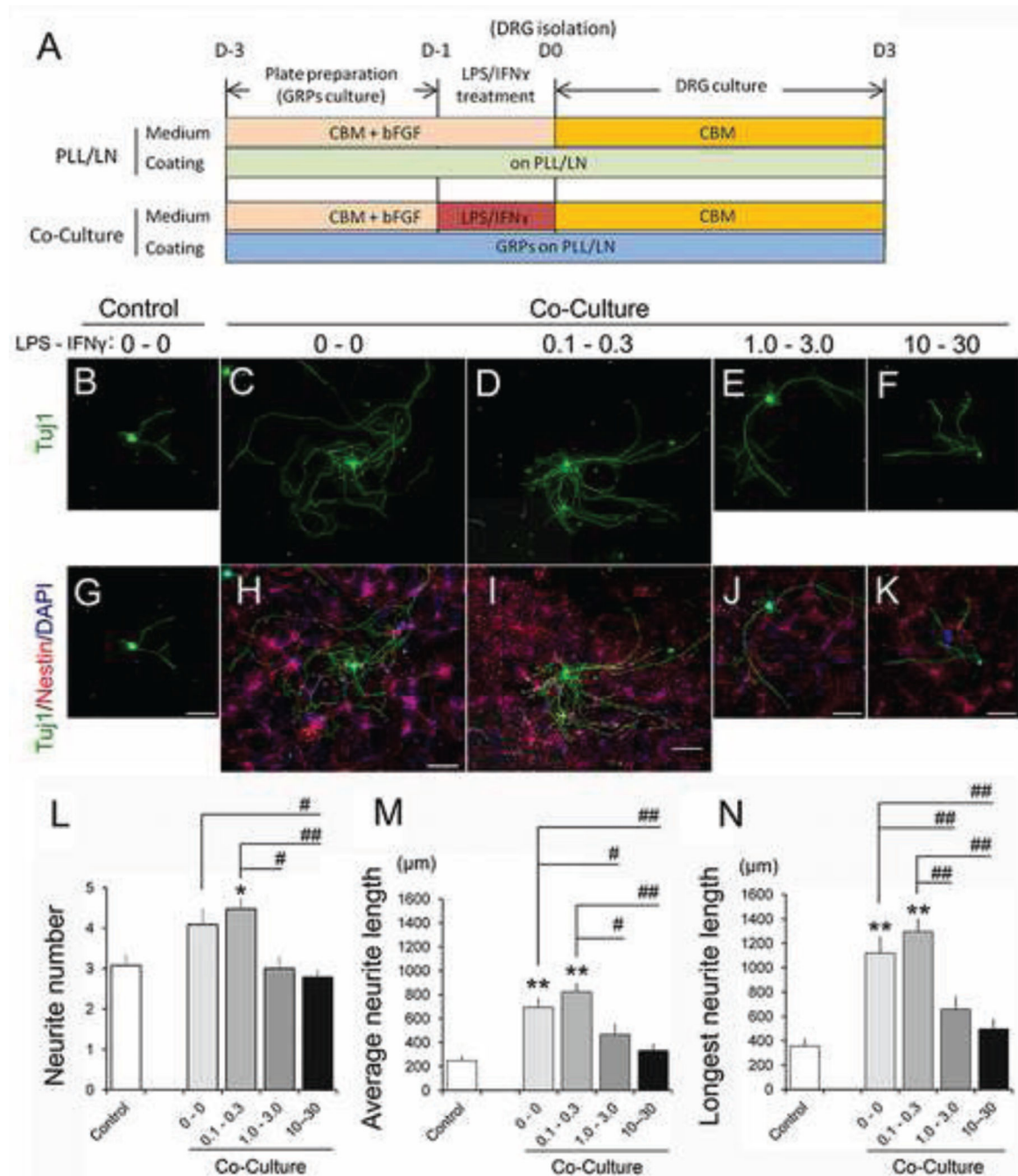


**Figure 5.** LPS/IFN $\gamma$  treatment altered GRP's promoting effect on neurite outgrowth from DRG in vitro. (A) Experimental design of co-culture with GRP treated with LPS/IFN $\gamma$ . (B-K) Immunostaining of DRG and DRG co-cultured with GRP treated with each concentration of LPS/IFN $\gamma$  ( $\mu$ g/ml-ng/ml). Upper panels: Tuj1 (DRG) (B-F), Lower panels: merge of Tuj1 and Nestin (GRP) (G-K). Scale bars = 150 $\mu$ m. Quantitative analysis of neurite outgrowth from DRG co-cultured with GRP treated with LPS-IFN $\gamma$  demonstrated that higher concentration of LPS-IFN $\gamma$  treatment (1.0-3.0 and 10-30 ( $\mu$ g/ml- ng/ml) attenuated GRPs'



promoting effect on neurite outgrowth in all parameters. (L) Primary neurite number, (M) average neurite length, and (N) longest neurite length. Asterisk represents significant difference relative to control (\*P<0.05, \*\*P<0.005). Sharp represents significant difference relative to correspondents among LPS-IFN $\gamma$  treated groups (#P<0.05, ##P<0.005). Experiments were repeated for three times and representative data are shown in Figure as mean  $\pm$  standard error of the mean (SEM). Statistical analysis was performed by one-way ANOVA with Bonferroni test. (N>30)

Author Manuscript

Author Manuscript

Author Manuscript

Author Manuscript

**Table 1**

Primary and secondary antibodies used in this study

Name	Type	Dilution	Source
A2B5	Mouse IgM	1:2	Hybrydoma
GFAP	Rabbit	1:2000	Chemicon
Vimentin	Mouse	1:1000	DAKO
Nestin	Mouse IgG1	1:1000	BD Pharmigen
MBP	Mouse IgG2b	1:1000	Invitrogen
Tuj1	Rabbit IgG	1:1000	Covance
Ki67	Rabbit IgG	1:200	ThermoFisher
goat $\alpha$ mouse-IgM RITC		1:400	Jackson
goat $\alpha$ mouse-IgG RITC		1:400	Jackson
goat $\alpha$ rabbit RITC		1:400	Jackson
goat $\alpha$ mouse-IgG FITC		1:400	Jackson
goat $\alpha$ rabbit FITC		1:400	Jackson

Author Manuscript

Author Manuscript

Author Manuscript

Author Manuscript